International Conference on Space Optics—ICSO 2004

Toulouse, France

30 March–2 April 2004
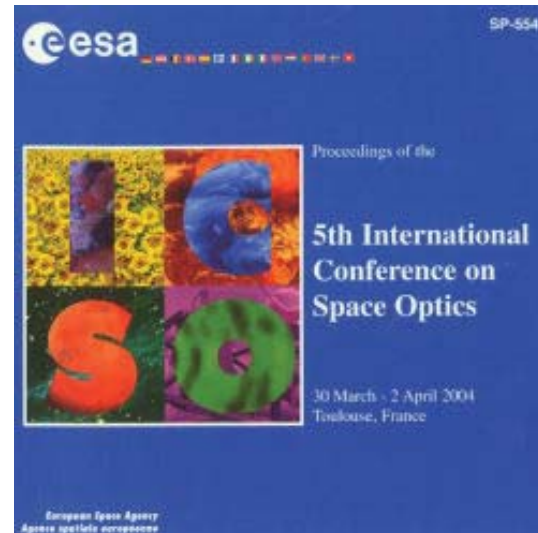
A starting point of an integrated optics concept for a space-based interferometer

Lucas Labadie, Pierre Kern, Isabelle Schanen

A STARTING POINT OF AN INTEGRATED OPTICS CONCEPT
FOR A SPACE-BASED INTERFEROMETER

Lucas LABADIE[(1)]**, Pierre KERN**[(1)]**, Isabelle SCHANEN**[(2)]**,**
[(1)] *LABORATOIRE D'ASTROPHYSIQUE DE GRENOBLE, BP53, 38041 Grenoble Cedex 9 – France*
E-mail : Lucas.Labadie@obs.ujf-grenoble.fr
E-mail : Pierre.Kern@obs.ujf-grenoble.fr
[(2)] *INSTITUT DE MICROELECTRONIQUE ET PHOTONIQUE, 38016 Grenoble Cedex 1 – France*
E-mail : Schanen@enserg.fr

ABSTRACT

This article deals with instrumentation challenges of the stellar interferometry mission *IRSI-Darwin* of the European Space Agency. The necessity to have a reliable and performant system for beam recombination has enlightened the advantages of an integrated optics solution, which is already in use for ground-base interferomety in the near infrared. However, since Darwin will operate in the mid infrared, this requires extending the integrated optics concept in this spectral range. This paper presents the guiding lines of the characterization work that should validate a new integrated optics concept for the mid infrared. We present also one example of characterization experiment we are working on.

1. INTRODUCTION

In terms of high angular resolution, long baseline interferometry represents a major research field that was explored and developed to a large scale in the last years [1]. To illustrate that, we know the highest spatial frequency achievable with a two aperture interferometer is proportional to B/λ where B is the projected baseline on the incident pane. If B is n times larger than the diameter of a monolithical telescope operating at its diffraction limit, we have the same order of magnitude between the angular resolutions of the two type of instrument. In order to operate as an imager, an interferometer provides the measurement of the contrast and the phase of the fringe pattern, which gives a *complex visibilty* at the specific spatial frequency B/λ. Following the *Van Cittert-Zernike* theorem, when the complex visibility distribution over the plane of spatial frequencies can be measured, its Fourier Transform gives under certain conditions an access to the intensity distribution of the observed source. Therefore, interferometry represents a way to image astronomical sources unresolved by a monolithic telescope. This fundamental property has then paved the way to the development of large interferometry array.

2. A NOVEL INSTRUMENTAL CONCEPT

In the past years was shown the importance of spatial filtering to remove the phase disturbance due either to atmosphere turbulence or to optical defects. This could be implemented by using pinhole, single-mode optical fibers or integrated optics (*IO*) components. This last solution also provides optical functions such as beam combination, photometric and polarization control [2]. Its advantage is then to gather several functions on a single and compact optical chip that provides stability, no alignment issues except for coupling and low sensitivity to external constraints. For a multi-aperture interferometer like *IRSI-Darwin* [3],[4] where stability and optical alignment are required, an *IO* solution can be a valuable alternative to a complex bulk optics recombination system.

To date, integrated optics for astronomy is limited to the near infrared windows *H* and *K* [5] due to the silica transmission window. Next step is, within the frame of an *ESA* contract, to study the way to extend the use of *IO* solutions to longer infrared wavelength and to develop, characterize and validate a first interferometric component for the *Darwin* band [4µm – 20µm].

3. TECHNOLOGICAL ISSUES

The development of integrated optics solutions is based on the waveguide theory that shows electromagnetic radiation can be confined under certain conditions into a guiding structure [6]. Since large literature is available on the mathematical approach of this problem, we will not treat those aspects in this paper. We will only remind here that light travels into the guiding structure are limited to a relatively small number of possible paths called modes. The number of those modes is closely linked to the dimensions of the structure, to the operating wavelength and to the refractive index distribution for dielectric waveguides.

With respect to what said previously, the extension of the integrated optics concept to the thermal infrared range is first of all a technological issue based on the availability of transparent material all over the Darwin range and on our ability to use them for specific

functions design in term of mechanical, structural and thermal behavior. The procedure that should lead to the development of a first IO component is an iterative process between two parts: on one side the technological work which identifies suitable microtechnology solutions to achieve a guiding structure and on the other side the characterization work that aims to determine the physical and optical parameters that will influence the performances of a specific technology. Some pertinent features that may constrain the performance of a waveguide are:

- Transmission spectral range that has to fill the Darwin band requirements.
- Modal behavior: the dimensioning of the waveguide and the refractive index distribution will set the single-mode spectral range.
- Overall losses, which are mainly separated into propagation losses, Fresnel losses and coupling losses.

We split the characterization phase into three parts that correspond to different levels of the project as shown in Tab. 1. For each phase we present the physical and optical parameters that need to be monitored. This requires the implementation of specific optical setups that we partially present hereafter.

4. CHARACTERIZATION METHODS IN THE THERMAL INFRARED

First step has been to identify from literature infrared bulk materials which show a good transmission for the entire specified band. In the context of this work, the technologies involved in the manufacturing process have led to select two types of glasses for the dielectric waveguide approach, which are Zinc Selenide (ZnSe) and Chalcogenide glasses. Fig.1. and Fig.2. provides the spectral transparency of the two materials. Both cover the entire $[4\mu m - 20\mu m]$ spectral range and comply then with the criterion on transmission.

A second approach has been also considered through the hollow metallic waveguide technology. In this case,
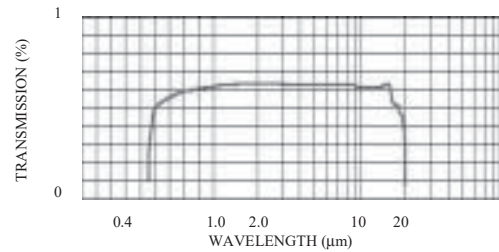

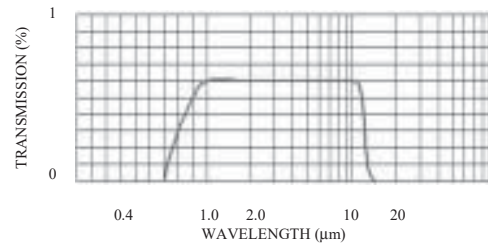Fig. 1. Spectral transmission of ZnSe glass (Janos Technology)

Fig. 2. Spectral transmission of AMTIR-1 chalcogenide glass (Janos Technology)

the successive metallic reflections confine light in the air core, which is transparent for the whole spectral range. Propagation losses induced in a hollow waveguide are mainly dependent on the reflectivity of the metallic coating [7]. Typical high-reflectivity coatings for the thermal infrared are Gold and Silver coatings.

Those considerations give the basic guidelines from a material point of view. The pre-selection of specific technologies to develop integrated optics waveguides is mainly based on the gained experience and knowledge on the material processes by the different institutes involved in the project.

4.1 Modal behavior of a waveguide

The modal behavior of a dielectric step-index waveguide is fully determined by its couple Δn – thickness. The index difference between the film and

Material characterization	Waveguide behavior	IOC characterization
Evaluation of the transparency window and losses - Transparency for bulk - Transparency for thin films - Complex refractive index - Metal reflectivity/absorption	*Characterization of planar structures and channel waveguides* - Single-mode behavior . Cut-off wavelength . Near field imaging - Propagation losses	*Characterization of IOC functions* - Overall losses - Fringes contrast measurements

Tab. 1: characterization parameters

the substrate will determine the guiding conditions. Low index difference will induce so-called "weak guiding conditions", which means an important part of the propagating field exist in the substrate and can be affected by its absorption along the waveguide length. A thicker film must then be deposited to allow modes propagation. High index difference will lead to a strong confinement of the electromagnetic film into the guide. This induces a smaller thickness of the film but increases the coupling issues.

In addition to that, we show that the number of propagating modes in a waveguide with given Δn and W decreases when the wavelength increases. For instance, a 10-modes waveguide at λ=0.632 μm will progressively loose its higher modes one by one with increasing wavelength. Above a certain value (called the cut-off wavelength), only the fundamental mode can propagate: we have a single-mode waveguide.

Considering those notions, we understand that we can return the problem and determine the index difference Δn (by choosing the appropriate materials) and the thickness W of the deposited film in order to obtain a single-mode waveguide at a specific wavelength (or range).

4.2   *M-lines* **method for samples characterization**

This method concerns only the dielectric waveguides. A short theoretical reminder is made before presenting this method. The propagation of light into a dielectric waveguide is characterized by a set of effective indexes. A given mode propagates into a gradient index waveguide with the wave vector given in Eq. 1.

$$k(x) = \omega\sqrt{\mu_0 \varepsilon(x)} = \sqrt{k_x^2(x) + k_z^2} \qquad (1)$$

The quantities $k_x(x)$ and k_z are the transverse and longitudinal component, μ_0 the vacuum permeability, $\varepsilon(x)$ the material permittivity distribution in the x direction. The refractive index can be written as in Eq.2

$$n^2(x) = \varepsilon(x) / \varepsilon_0 \qquad (2)$$

and Eq. 1 can be rewritten

$$k_0^2(x).n^2(x) = k_x^2(x) + k_z^2 \qquad (3)$$

The quantity k_x^2/ k_0^2 is defined as the effective index n_{eff} of the mode, which can be interpreted as the refractive index "seen" by a plane wave corresponding to a specific mode and propagating along the z axis. In the geometrical approach of electromagnetic waves propagation, the angle of the propagating ray $\theta(x)$

measured with respect to the z axis is obtained from Eq. 4

$$\cos \theta(x) = \frac{k_z}{k(x)} = \frac{k_z}{k_0 n(x)} \qquad (4)$$

and thus we have

$$n_{eff} = n(x)\cos \theta(x) \qquad (5)$$

The propagation constant is given in Eq. 6.

$$\beta = k.n_{eff} \qquad (6)$$

Solving the Maxwell's equation in the waveguide succeeds to discrete solutions for the propagation constant, results in discrete solutions for the effective index as well.

The principle of the *m-lines* method is to excite with a monochromatic radiation the different modes of a slab waveguide sample using a prism coupling technique. Fig. 3 shows the principle of the experiment.
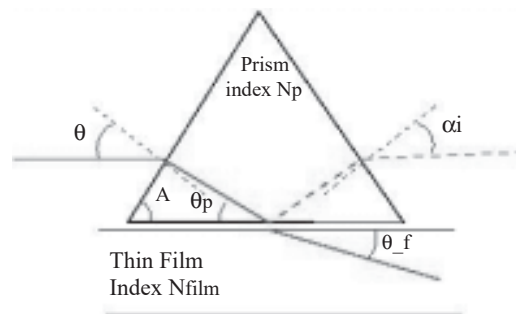

Fig. 3. Principle of the m-lines method

When a prism is placed on the surface of a slab waveguide and we have an incident beam in total reflection conditions at the base of the prism, theory shows that light can be coupled through the evanescent field existing in the air gap between the layer and the prism base if the phase matching conditions of Eq.7 [6] are fulfilled.

$$n_p \cos(\theta_p) = n_{film} \cos(\theta_{film}) \qquad (7)$$

The quantities n_p and n_{film} are the refractive index of the coupling prism and the thin layer. θ_p and θ_{film} are the beam angular direction. In those conditions, rays of the focalized input beam filling the phase matching conditions will be coupled into the waveguide and "black lines" will be detected at discrete angular

positions α_i. From the measurement of α_i, we retrieve the corresponding mode effective index through Eq.8.

$$n_{eff} = n_p \, \sin(\arcsin(\frac{\sin(\alpha_i)}{n_p}) - A) \qquad (8)$$

A is the angular aperture of the prism, n_p its refractive index. Note that in order to excite successive modes from the fundamental one, it is necessary to use a coupler with higher index with respect to the film to be characterized. This can be checked out knowing the refractive index of film bulks since the index of the thin film will be lower than the bulk material. The method gives access to the set of effective indexes of the waveguide (called also mode indexes). Processing those data allows retrieving the index profile and the thickness of the waveguide.

For gradient index stuctures, the index profile can be retrieve using the original procedure proposed by White [8] and based on the WKB method. Index profile n(x) for TE modes is computed solving Eq.9.

$$2k \int_0^{x(m)} \sqrt{n(x)^2 - n_{eff}^2(m)} \, . dx = 2m\pi + 2\phi_0 + 2\phi_1 \qquad (9)$$

Quantity x(m) is the turning point in a gradient index waveguide, m is the mode number, $n_{eff}(m)$ is the effective index of mode m and k the modulus of the wave vector. ϕ_0 and ϕ_1 are the phase changes at the turning points x(m) and -x(m) which are taken equal to $\pi/4$ in [8]. In our study, we have an *a priori* knowledge that the index profile is a step. The method to retrieve the film index is then slightly changed. Phase changes computed at waveguide-air and waveguide-substrate interfaces are different due to sharp change in index. In [9], Tien *et al.* solved the equation

$$2.k.W . \sqrt{n_{film}^2 - n_{eff}^2(m)} = 2m\pi + 2\phi_0 + 2\phi_1 \qquad (12)$$

where W is the film thickness. ϕ_0 and ϕ_1 are the phase shifts respectively at the air-film and film-substrate interface. Knowing two effective indexes, we compute the index n_{film} and then the thickness W.

4.3   Characterization in the visible and NIR

Considering what previously said, we start to characterize samples in the visible and near infrared (NIR) where a multimode behavior is expected. The advantage of this procedure is to extract the thickness of the thin layer which is constant with respect to the wavelength. We characterize two type of samples which are AMTIR-1 (Chalcogenide glass) and Zinc Selenide (ZnSe) films. Fig.1 and Fig.2 show they are

suitable for measurement from visible to mid-infrared range. ZnSe is deposited on Zinc Sulfide (ZnS) substrate while AMTIR-1 is deposited on a silica substrate. We proceed to measurements at $\lambda=0.632\mu m$ and $\lambda=1.323\mu m$. As a coupler we use a TiO_2 prism with indexes n=2.864 at $0.632\mu m$ and n=2.715 at $1.323\mu m$ with TE polarization. The prism aperture is A=45.1458°. In Tab.2. are given the bulk indexes of the substrate used for computation.

TE	Lambda (μm)	ZnS	Silica
	0.632	2.352	1.457
	1.323	2.289	1.449

Tab.2 : index of the substrates

The measurements are carried out with a broadband source placed behind a monochromator to select the desired wavelength. We report in Tab.3 and Tab.4 the experimental values of effective indexes for the near infrared for AMTIR-1 and ZnSe films.

Mode m	Angle α_i	$n_{eff}(m)$	Error on α_i
0	-33.97	2.277	+0.01
1	-30.87	2.252	-
2	-24.48	2.194	-
3	-16.69	2.116	-
4	-6.74	2.005	-
5	4.26	1.871	-

Tab.3 : Angular position of TE guided modes for AMTIR-1 sample on silica substrate at $\lambda=1.323\mu m$

Mode m	Angle α_i	$n_{eff}(m)$	Error on α_i
2	-50.43	2.389	+0.01
3	-42.93	2.343	-
4	-35.37	2.288	-
5	-27.62	2.223	-
6	-19.62	2.147	-
7	-11.22	2.057	-

Tab.4 : Angular position of TE guided modes for ZnSe sample on ZnS substrate at $\lambda=1.323\mu m$

Based on Eq.12, we compute the refractive index and thickness of the films. For the chalcogenide sample we obtain n_{TE} =2.301 ± 0.0011 and e=2.98μm ± 0.014. For the ZnSe sample we obtain n_{TE} =2.441 ± 0.0012 and e=3.83μm ± 0.033.

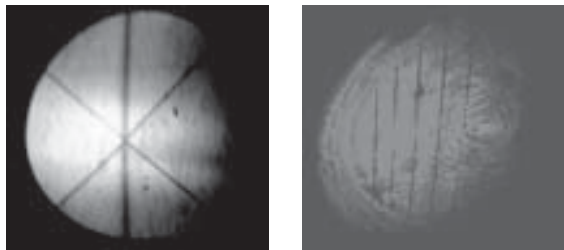In Fig.5, we show an example of m-lines outputs obtained during the measurements

Fig. 5. M-lines outputs for a chalcogenide slab
waveguide at 1.3 μm (left) and 0.632μm (right)

4.4 Characterization in the thermal infrared

Previous measurements on ZnSe sample have shown
that this structure, initially designed for the mid-
infrared range, is suitable for guidance and that there is
no important drawbacks on the technology. It has also
permitted to measure the film thickness, which will be
used for later measurement in the thermal infrared.

Indeed, since we expect to be single-mode at 10.6μm,
we obtain a single line: therefore the knowledge on the
film thickness is mandatory to compute the refractive
index according to Eq.12. The setup we implement in
the frame of our project uses the 10.6 μm line of a CO2
laser. We use a Germanium prism with n=4.0 and
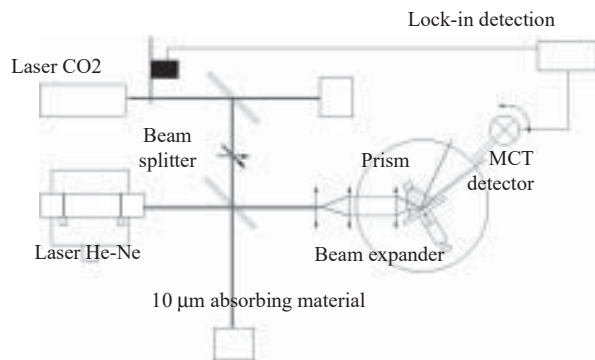A=45°. The layout of the setup is shown in Fig.6.

Fig. 6. The m-lines setup for mid-infrared

This setup has been developed at LAOG and is to date
under validation. Next step is to complete the phase
with a measurement at 10.6μm and eventually extend
it to other pertinent wavelength of the *Darwin* band.

5. CONCLUSION

The characterization phase for the extension of the
integrated optics concept to the thermal infrared range
has started with first index measurements using the *M-
lines* experiment. Although they were not presented

here for sake of shortness, other characterization
methods are being implemented to have a complete set
of test benches for mid-infrared integrated optics.

6. ACKNOWLEDGMENTS

7. REFERENCES

1. Peter R. Lawson, *Principles of Long Baseline
Stellar Interferometry*, Course notes from the 1999
Michelson Summer School

2. P. Kern, I. Schanen, *Integrated optics single-mode
interferometric beam combiner for near infrared
astronomy*, Integrated Optics for Astronomical
Interferometry, Eds. P.Kern & F.Malbet, pp 15,
1997

3. A. Léger, J.M. Mariotti, M. Ollivier, *Could we
search for primitive life on extrasolar planets in
the near future? The Darwin Project*, Icarus 123,
pp 249-255, 1996

4. R.L. Bracewell, R.H. MacPhie, *Searching for
nonsolar planets*, Icarus 38, pp 136-147, 1979

5. J-P. Berger, P. Haguenauer, P. Kern, *Integrated
Optics for Astronomical Interferometry – First
measurements of stars*, Astronomy & Astrophysics
376, pp 31-34, 2001

6. D.L. Lee, *"Electromagnetic Principles of
Integrated Optics"*, Wiley, New York, 1986

7. F.E. Vermeulen, C.R. James, A.M. Robinson,
*Hollow microstructural waveguides for
propagation of infrared radiation,* Journal of
Lightwave Technology 9, pp 1053-1059, 1991

8. J.M. White, P.F. Heidrich, *Optical waveguide
refractive index determined from measurements of
mode indexes: a simple analysis*, Applied Optics
15, pp. 151-155, 1976

9. P.K. Tien, R. Ulrich, R.J. Martin, *Modes of
propagating light waves in thin deposited
semiconductor,* Applied Physics Letters 14, pp.
291-294, 1969